Original Article

# Prognostic value of nicotinamide adenine dinucleotide ($NAD^+$) metabolic genes in patients with stomach adenocarcinoma based on bioinformatics analysis

**Linkun Cai[1#^], Chuanfeng Ke[2#], Zikai Lin[3#], Yalan Huang[4], Aling Wang[1], Shiying Wang[1], Chunhui Chen[1], Cailing Zhong[1], Lingyu Fu[1], Peixin Hu[1], Jiwei Chai[1], Haiyan Zhang[1], Beiping Zhang[1]**

[1]Department of Gastroenterology, The Second Affiliated Hospital of Guangzhou University of Chinese Medicine, Guangzhou, China; [2]Department of Gastrointestinal Surgery, The First Affiliated Hospital of Guangzhou Medical University, Guangzhou, China; [3]Nanshan School, Guangzhou Medical University, Guangzhou, China; [4]Hunan University of Chinese Medicine, Changsha, China

*Contributions:* (I) Conception and design: B Zhang, H Zhang; (II) Administrative support: B Zhang, H Zhang, C Ke; (III) Provision of study materials or patients: L Cai, C Ke, Z Lin; (IV) Collection and assembly of data: L Cai, C Ke, Z Lin; (V) Data analysis and interpretation: L Cai, C Ke, Z Lin; (VI) Manuscript writing: All authors; (VII) Final approval of manuscript: All authors.

[#]These authors contributed equally to this work.

*Correspondence to:* Beiping Zhang; Haiyan Zhang. Department of Gastroenterology, The Second Affiliated Hospital of Guangzhou University of Chinese Medicine, 111 Dade Road, Yuexiu District, Guangzhou 510120, China. Email: doctorzbp@163.com; zhanghaiyan128@126.com.

**Background:** Because stomach adenocarcinoma (STAD) has a poor prognosis, it is necessary to explore new prognostic genes to stratify patients to guide existing individualized treatments.

**Methods:** Survival and clinical information, RNA-seq data and mutation data of STAD were acquired from The Cancer Genome Atlas (TCGA) database. Fifty-one nicotinamide adenine dinucleotide ($NAD^+$) metabolism-related genes (NMRGs) were obtained from the Kyoto Encyclopedia of Genes and Genomes (KEGG) and Reactome databases. Differentially expressed NMRGs (DE-NMRGs) between STAD and normal samples were screened, and consistent clustering analysis of STAD patients was performed based on the DE-NMRGs. Survival analysis, Gene Set Enrichment Analysis (GSEA), mutation frequency analysis, immune microenvironment analysis and drug prediction were performed among different clusters. Additionally, the differentially expressed genes (DEGs) among different clusters were selected, and the intersections of DEGs and DE-NMRGs were selected as the prognostic genes. Finally, quantitative real-time polymerase chain reaction (qRT-PCR) was performed on a human gastric mucosa epithelial cell line and cancer cell line to verify the expression of the prognostic genes.

**Results:** A total of 27 DE-NMRGs and two clusters were selected. There was a difference in survival between clusters 1 and 2. Furthermore, 18 DE-NMRGs were significantly different between clusters 1 and 2. The different Gene Ontology (GO) biological processes and KEGG pathways between clusters 1 and 2 were mainly enriched in cyclic nucleotide mediated signaling, synaptic signaling and hedgehog signaling pathway, etc. The somatic mutation frequencies were different between the two clusters, and TTN was the highest mutated gene in the patients of the clusters 1 and 2. Additionally, eight immune cells, immune score, stromal score, and estimate score were different between clusters 1 and 2. The patients in cluster 2 were sensitive to CTLA4 inhibitor treatment. Furthermore, the top five drugs (AP.24534, BX.795, Midostaurin, WO2009093927 and CCT007093) were significantly higher in cluster 1 than in cluster 2. Finally, three genes (AOX1, NNMT and PTGIS) were acquired as prognostic, and their expressions were consistent with the results of bioinformatics analysis.

**Conclusions:** Three prognostic genes related to $NAD^+$ metabolism in STAD were screened out, which provides a theoretical basis and reference value for future treatment and prognosis of STAD.

^ ORCID: 0000-0003-2036-1797.

 

**Keywords:** Stomach adenocarcinoma (STAD); nicotinamide adenine dinucleotide metabolism (NAD+ metabolism); prognosis

Submitted Sep 26, 2022. Accepted for publication Nov 24, 2022.
doi: 10.21037/jgo-22-1092
**View this article at:** https://dx.doi.org/10.21037/jgo-22-1092

## Introduction

Gastric cancer (GC) is a malignant tumor originating from the gastric mucosal epithelium, and is often hidden, without specific symptoms. The incidence of GC in males is higher than in females, and worldwide it has become the fourth leading cause of death (1). The most common histological type of GC is stomach adenocarcinoma (STAD), which accounts for about 95% of GC patients. Research data show that in 2020 there were about 1.09 million new cases of GC in the world, and about 769,000 GC patients died (1). The mechanism of the occurrence and development of STAD is not completely clear. Patients usually seek treatment for dyspeptic symptoms such as nausea and vomiting, and the diagnosis is usually in the middle and late stages (2-4). In recent years, the incidence of GC has decreased, but the prognosis is not good. Therefore, it is necessary to explore new prognostic genes for stratified analysis of patients to guide the existing individualized therapy.

Nicotinamide adenine dinucleotide ($NAD^+$) is one of the most important coenzymes in redox reactions and the core of energy metabolism. The traditional concept describes nicotinamide nucleotide metabolism as a very static process, which mainly emphasizes the mutual transformation between NAD and NADP oxidation and reduction forms (5,6). However, studies over the past 30 years have clearly shown that the metabolism, transport and function of NAD are dynamic and complex. NAD can be converted into NADP, NAADP and cADPR, which play key roles in energy transduction and cellular signal transduction, and the degradation products of NAD, such as nicotinamide and N-methylnicotinamide, have also been considered as key regulators of energy metabolism, epigenetics and disease status (7,8). NAD pathway metabolites can also be used as substrates for a variety of enzymes, including PARPs, sirtuins, CD38, ART, SARM1 and RNA polymerase, which are involved in many aspects of cell homeostasis (9,10). There are three independent metabolic pathways of $NAD^+$ in the human body: Preiss-Handler pathway, ab initio synthesis pathway and remedial synthesis pathway (11). Changes in NAD homeostasis can be found in age-related diseases such as neurological diseases, diabetes, and cancer (12). The NAMPT-mediated remedial pathway is necessary for most $NAD^+$ production in mammalian cells, and the latest research by Lv *et al.* proposed that NAMPT, a key rate-limiting enzyme in the $NAD^+$ synthesis pathway, be used as a starting point. It was found that $NAD^+$ metabolism can drive tumor immune escape in a $CD8^+$ T cell-dependent manner (13), suggesting that the level of $NAD^+$ or NAMPT should also predict the effect of immunotherapy to some extent.

Therefore, in this study we downloaded the data of gastric adenocarcinoma patients from the University of California Santa Cruz (UCSC) Xena and carried out molecular stratification analysis based on $NAD^+$ metabolism-related genes (NMRGs) to evaluate the relationship between different clusters and the prognosis of STAD, in order to further understand the differences *in vivo* of STAD patients with different survival rates. We present the following article in accordance with the REMARK reporting checklist (available at https://jgo.amegroups.com/

### Highlight box

**Key findings**

- Three nicotinamide adenine dinucleotide metabolism-related genes were discovered to play an important role in STAD.

**What is known and what is new?**

- $NAD^+$ can directly and indirectly affect several essential biological activities, including metabolic pathways, DNA repair, chromatin remodeling, cellular senescence, and immune cell function.
- The kynurenine metabolic pathway affected by the key gene *AOX1* is a potential target for the treatment of gastric adenocarcinoma, and it may be possible to improve the efficacy of gastric adenocarcinoma immunotherapy by inhibiting kynurenine metabolism.

**What is the implication, and what should change now?**

- Our results provide a theoretical basis and reference value for the treatment and prognosis of STAD. More research is needed to gain insight into the role of NMRGs in tumor development and to elucidate these molecular mechanisms that are of great value for cancer therapies targeting $NAD^+$ and its metabolites.

 

article/view/10.21037/jgo-22-1092/rc).

## Methods

### *Data sources*

Normalized gene expression data from RNA-sequencing (RNA-seq; Fragments Per Kilobase Million [FPKM] value) and somatic mutation data as well as the relevant clinical data of The Cancer Genome Atlas stomach adenocarcinoma (TCGA-STAD) cohort were downloaded from the University of California Santa Cruz (UCSC) Xena database (https://xenabrowser.net/datapages/, updated to July 20, 2019). The RNA-seq data contained 375 cancer and 32 normal samples, as well as 350 cancer samples with survival and clinical information. The NMRGs were downloaded from the "Pathway (hsa00760): Nicotinic acid and nicotinamide metabolism" metabolic pathway and the "R-HSA-196807: Nicotinic acid metabolism" metabolic pathway in the Kyoto Encyclopedia of Genes and Genomes (KEGG) database (https://www.kegg.jp/) and the Reactome database (https://reactome.org/) respectively according to a previous reference (14). Finally, 51 NMRGs were obtained after deduplication. The study was conducted in accordance with the Declaration of Helsinki (as revised in 2013).

### *Screening for DE-NMRGs and consistent cluster analysis*

A total of 49 NMRGs were identified in the RNA-seq data of STAD. The expression matrices of the 49 NMRGs were used to draw a boxplot using the R package "ggplot2" (15), and the differentially expressed NMRGs (DE-NMRGs) between STAD and normal samples were screened by the Wilcoxon test with $P<0.05$. The R package "ConsensusClusterPlus" (16) was used to perform consistent clustering analysis of STAD patients with the clustering parameters maxK =10, clusterAlg = "pam" and distance = "pearson", based on the DE-NMRGs. Next, the optimal clustering method was selected based on the boundary points where the cumulative distribution function (CDF) value changed the most and the CDF downward trend was more stable. The uniform manifold approximation and projection (UMAP) and principal component analysis (PCA) were used to evaluate the distribution between the clusters.

### *Survival analysis of patients with different clusters*

Survival analysis of the patients in each cluster was performed using the R package "survival" (17) to compare the differences in survival among patients in the different clusters. Boxplots of the DE-NMRGs expression levels between different isoforms were plotted by the Wilcoxon test using the R package "ggplot2" (15).

### *Correlation analysis between different clusters and clinical characteristics*

The correlation of clinical characteristics between different clusters was based on the clinical information of samples from the TCGA database and the different clusters of patients by Chi-square test. Next, the R package "Heatmap" was used to draw a heatmap of the clinical characteristics of different clusters and DE-NMRGs.

### *Gene set enrichment analysis (GSEA) functional enrichment analysis among different clusters*

The GSEA software (V4.0.3) was used to perform the functional enrichment analysis of the different clusters (18). The following parameters were set: (I) the KEGG pathway gene set was used as the enrichment background, setting the parameter gene sets database: c2.cp.kegg.v7.4.symbols.gmt; (II) the Gene Ontology (GO) biological process gene was set as the enrichment background, setting the parameter gene sets database: c5.go.bp.v7.4.symbols.gmt; (III) set different clusters as the phenotype file, setting the parameter phenotype label: cluster2 VS cluster1; (IV) set the parameter Metric for gene sorting: Signal2Noise; (V) set parameters: gene list sorting method: real, gene list sorting method: descending order. According to the different folds of the cluster 2 versus cluster 1, the above gene sets were used as background genes for enrichment analysis.

### *Analysis of somatic mutation among different clusters*

To investigate the somatic mutation frequencies among the different STAD clusters and observe different mutational patterns between clusters, the R package "maftools" was applied to analyze and visualize the mutation frequency of each mutation type between clusters (19). Single nucleotide variants (SNVs), single nucleotide polymorphisms (SNPs), insertions (INS), deletions (DELs) and other somatic mutational signatures between clusters were analyzed and visualized by "maftools" (19). Moreover, the top 20 genes with mutation frequencies in different clusters were selected for waterfall plot display. Next, the differentially mutated

 

genes between the different clusters were compared with P<0.001 by Fisher's test in the mafCompare function, and the forestPlot function to draw a forest plot for visualization.

### *Immune microenvironment analysis*

The proportion of 22 immune cells in all samples in the expression matrix was calculated using the Cell type Identification By Estimating Relative Subsets Of RNA Transcripts (CIBERSORT) and the LM22 gene set (20). CIBERSORT was used to calculate the proportion of each immune cell in each sample, and the corresponding statistical value was calculated, excluding samples with P>0.05 (20). Using the R package "ggplot2" to draw a violin plot by the Wilcoxon test based on the score of each immune cell, immune scores, stromal scores and estimate scores for different clusters which were calculated using the Estimate algorithm (21). The heatmap of immune scores, stromal scores, estimate scores and differential immune cell expression levels for different clusters was drawn using the R package "pheatmap" (22).

### *Sensitivity analysis of immunotherapy and predictive analysis of chemotherapeutics*

The sensitivities of PD-1 and CTLA4 inhibitors in the different clusters were analyzed using the submap algorithm in the GenePattern cloud server, and heatmaps were plotted by "pheatmap" (22). Based on the Genomics of Drug Sensitivity in Cancer database, a ridge regression model was constructed to predict each drug's IC50, and the IC50 of patients with different clusters of 136 drugs was predicted using the pRRophetic algorithm (23). Next, the R package "ggplot2" was used to draw boxplots for visualization. The Wilcoxon test method was used to screen out drugs with significant differences between clusters.

### *Screening for prognostic genes and prognostic analysis*

The differentially expressed genes (DEGs) in the gene expression matrix of different clusters were analyzed using the limma package (24). The difference threshold was set to: P<0.05 and |log2 fold change (FC)|>0.5. The intersections of the DEGs and DE-NMRG were selected as the prognostic genes using jVenn.

### *Quantitative real-time polymerase chain reaction (qRT-PCR)*

Human gastric mucosa epithelial cell line (GES-1) and three human gastric cancer cell lines (HGC-27, NCI-N87 and SNU-1) were purchased from iCell Bioscience Inc (Shanghai, China). Total RNA of all cell lines was extracted by TRIzol reagent (Thermo Fisher, ShangHai, CN). The sweScript RT I First strabd cDNA SynthesisAll-in-OneTM First-Strand cDNA Synthesis Kit (Servicebio, Wuhan, China) was used for reverse transcription to form cDNA. Finally, polymerase chain reactions (PCR) were performed with the 2× Universal Blue SYBR Green qPCR Master Mix (Servicebio). The primers of the prognostic genes were: AOX1-F: GTTCACATTTATCTTGATGGCTCTG, AOX1-R: GACATTCGACATTGGCATTCTTA; NNMT-F: CTCCTCTCTGCTTGTGAATCCT, NNMT-R: CCTGTCTCAACTTCTCCTCCTT; PTGIS-F: CTGGTTGGGGTATGCCTTGG, PTGIS-R: TCATCACTGGGGCTGTAATGT.

### *Statistical analysis*

All analyses were conducted using R language (https://www.r-project.org/). Differences in differentially expressed analysis, immune-related analysis, and drug sensitivity analysis between cluster 1 and cluster 2 were calculated by Wilcoxon test. For the clinical correlation analysis, the data from different clusters with different characteristics was compared by Chi-square test. The differentially mutated genes between the different clusters were compared by Fisher's test. If not specified above, P<0.05 was regarded as statistically significant.

## Results

### *Screening for DE-NMRGs and consistent cluster analysis*

A total of 27 DE-NMRGs were selected, including 11 downregulated DE-NMRGs and 16 upregulated DE-NMRGs (*Figure 1A*). Based on these 27 DE-NMRGs, two clusters were the best clusters with K =2 (*Figure 1B,1C*). The results of UMAP and PCA indicated that the distribution of the two clusters was clearer (*Figure 1D,1E*).

 

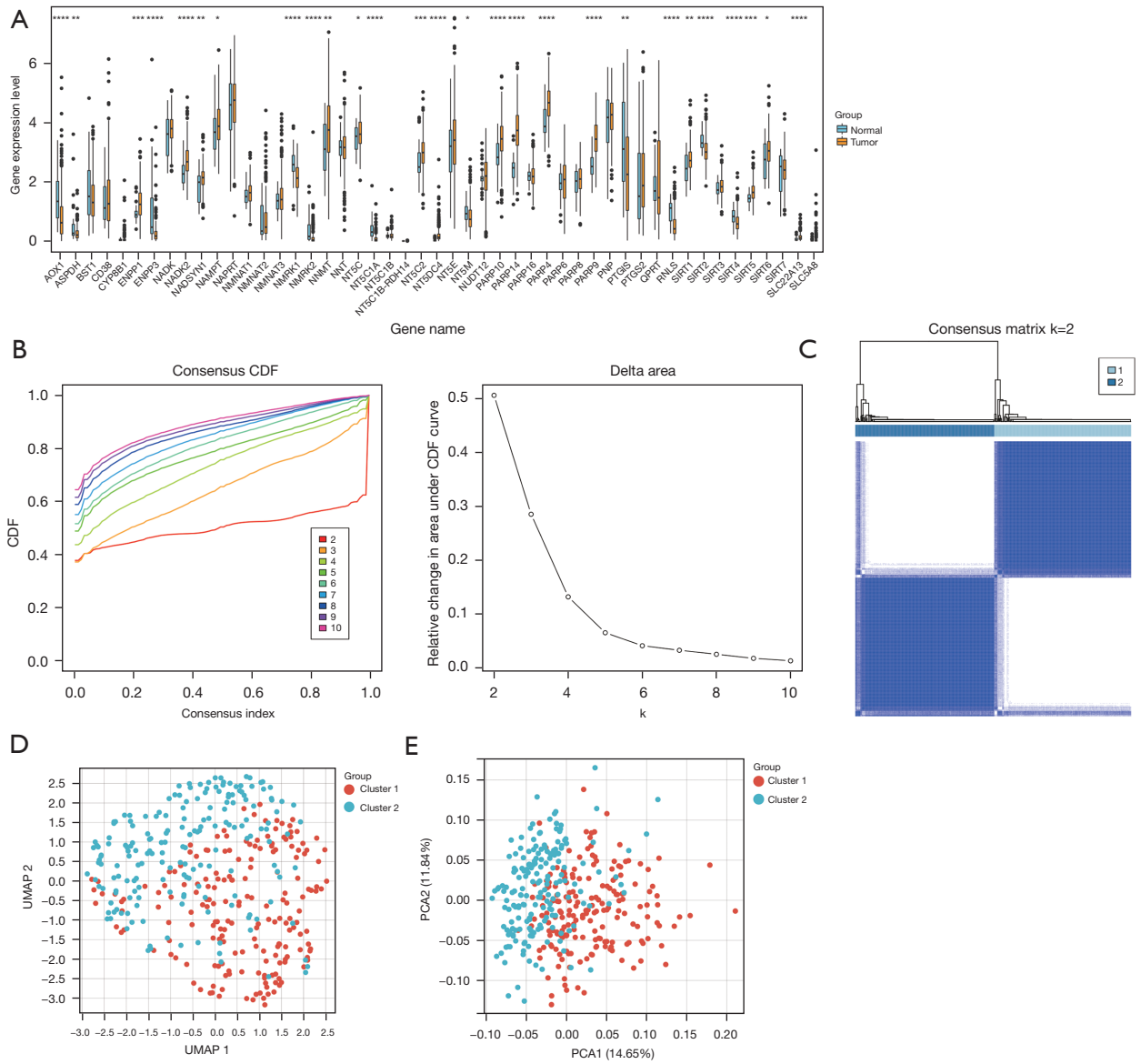


**Figure 1** Screening for DE-NMRGs and consistent cluster analysis. (A) Differentially expressed NAD$^+$ metabolic genes between cancer and normal samples. (B) Consensus clustering cumulative distribution function for k=2 to 10. (C) Consensus clustering matrix for k=2. (D) UMAP analysis confirmed the classification. (E) PCA analysis confirmed the classification. *, P<0.05; **, P<0.01; ***, P<0.001; ****, P<0.0001. CDF, cumulative distribution function; UMAP, uniform manifold approximation and projection; PCA, principal component analysis; DE-NMRGs, differentially expressed NAD$^+$ metabolism-related genes; NAD$^+$, nicotinamide adenine dinucleotide.

### *Survival analysis among patients with different clusters*

To compare the differences in survival between patients with different clusters, the Kaplan-Meier curves of the two clusters were drawn. There was a significant difference in survival between clusters 1 and 2 (P=0.025), with the patients in cluster 1 having a good prognosis (*Figure 2A*). Furthermore, 18 DE-NMRGs were significantly different between clusters 1 and 2, including *AOX1*, *ASPDH* and *ENPP1* (*Figure 2B*).

### *Correlation analysis between different clusters and clinical characteristics*

To understand the correlation between different clusters and clinical features, the clinical information of samples

 

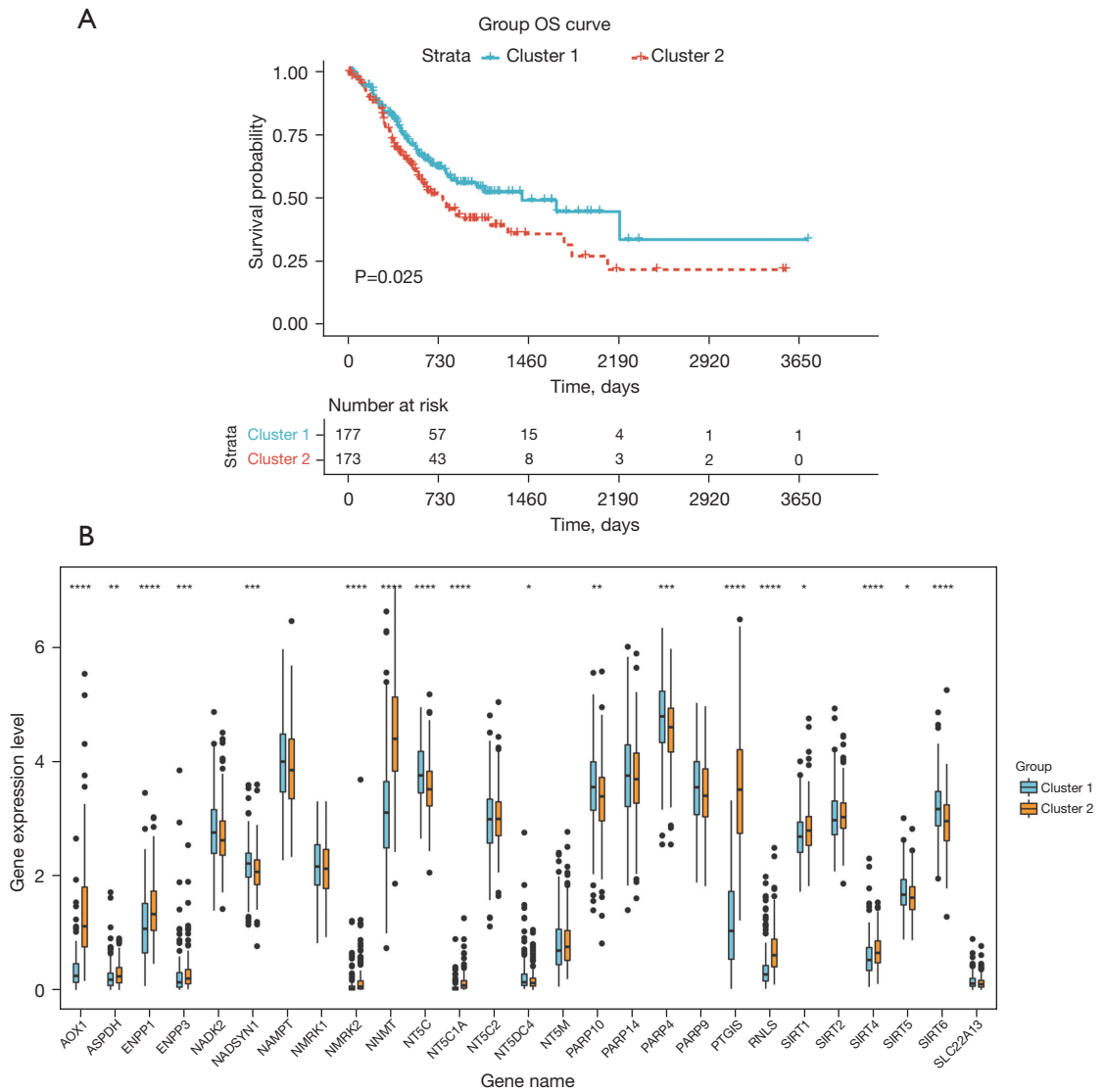


**Figure 2** Survival analysis among patients with different clusters. (A) Kaplan-Meier survival analysis for patients with STAD in two clusters. (B) Differentially expressed NAD+ metabolic genes between cluster 1 and cluster 2. *, P<0.05; **, P<0.01; ***, P<0.001; ****, P<0.0001. OS, overall survival; STAD, stomach adenocarcinoma; NAD+, nicotinamide adenine dinucleotide.

was combined with different clusters of patients from the TCGA database and clinical features that were significantly different from the different clusters were screened out. The neoplasm histologic grade (P=0.0020), OS (P=0.0430), pathologic T (P=0.0004) and tumor stage (P=0.0035) all significantly correlated with the different clusters (*Figure 3*, Figure S1).

### *GSEA functional enrichment analysis among different clusters*

The different GO biological processes and KEGG pathways between clusters 1 and 2 were enriched, respectively. The mainly GO terms enriched were cyclic_nucleotide_mediated_signaling (ES =0.6320), synaptic_signaling (ES =0.5450), regulation_of_dna_directed_dna_

 

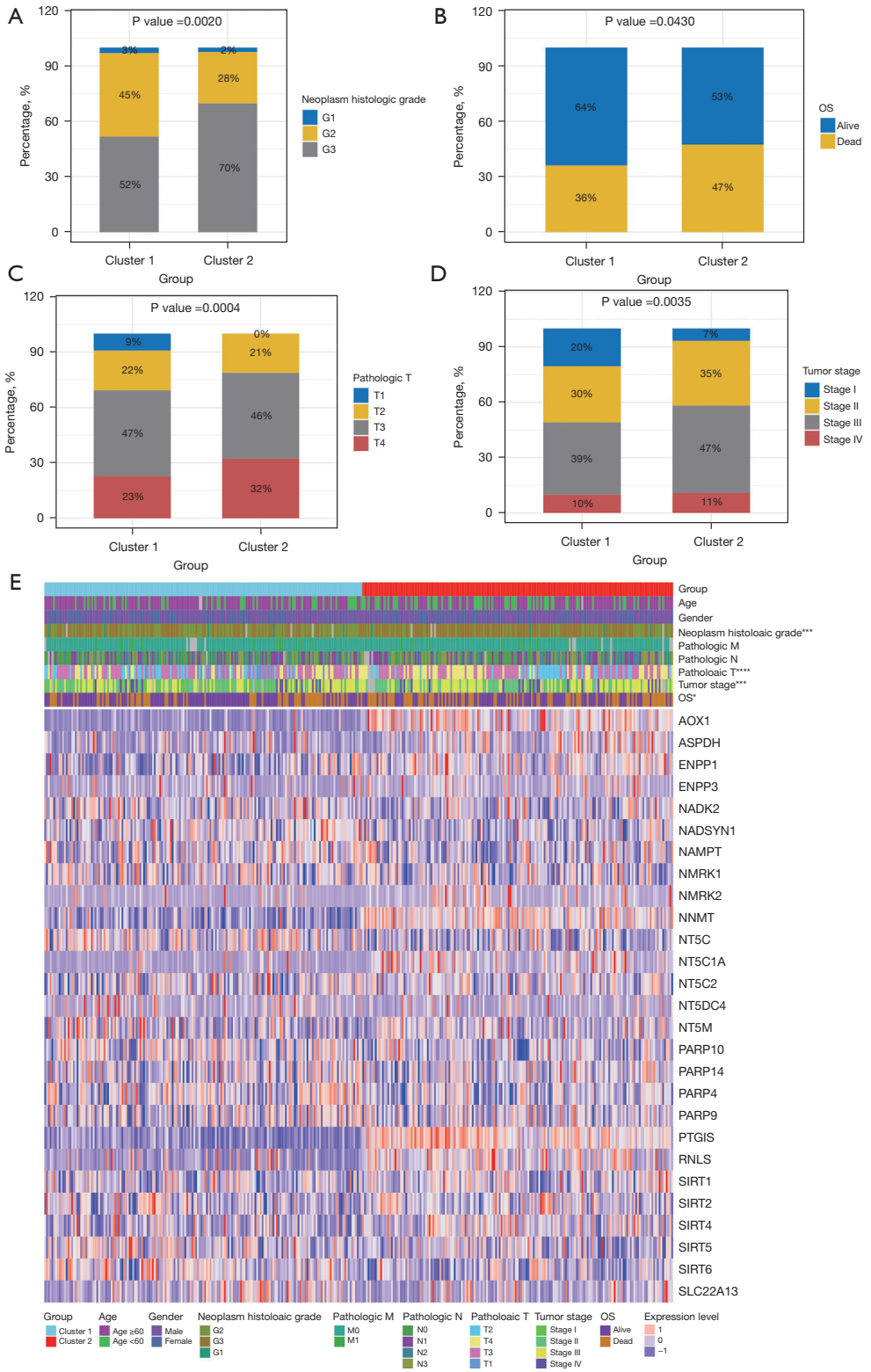


**Figure 3** Correlation analysis between different subtypes and clinical characteristics. (A) Neoplasm histologic grade. (B) OS. (C) Pathologic T stage. (D) Tumor stage. (E) Expression heatmap of clinical features and differential NMRGs in different subtypes. *, P<0.05; ***, P<0.001; ****, P<0.0001. OS, overall survival; NMRG, $NAD^+$ metabolism-related gene; $NAD^+$, nicotinamide adenine dinucleotide.

 

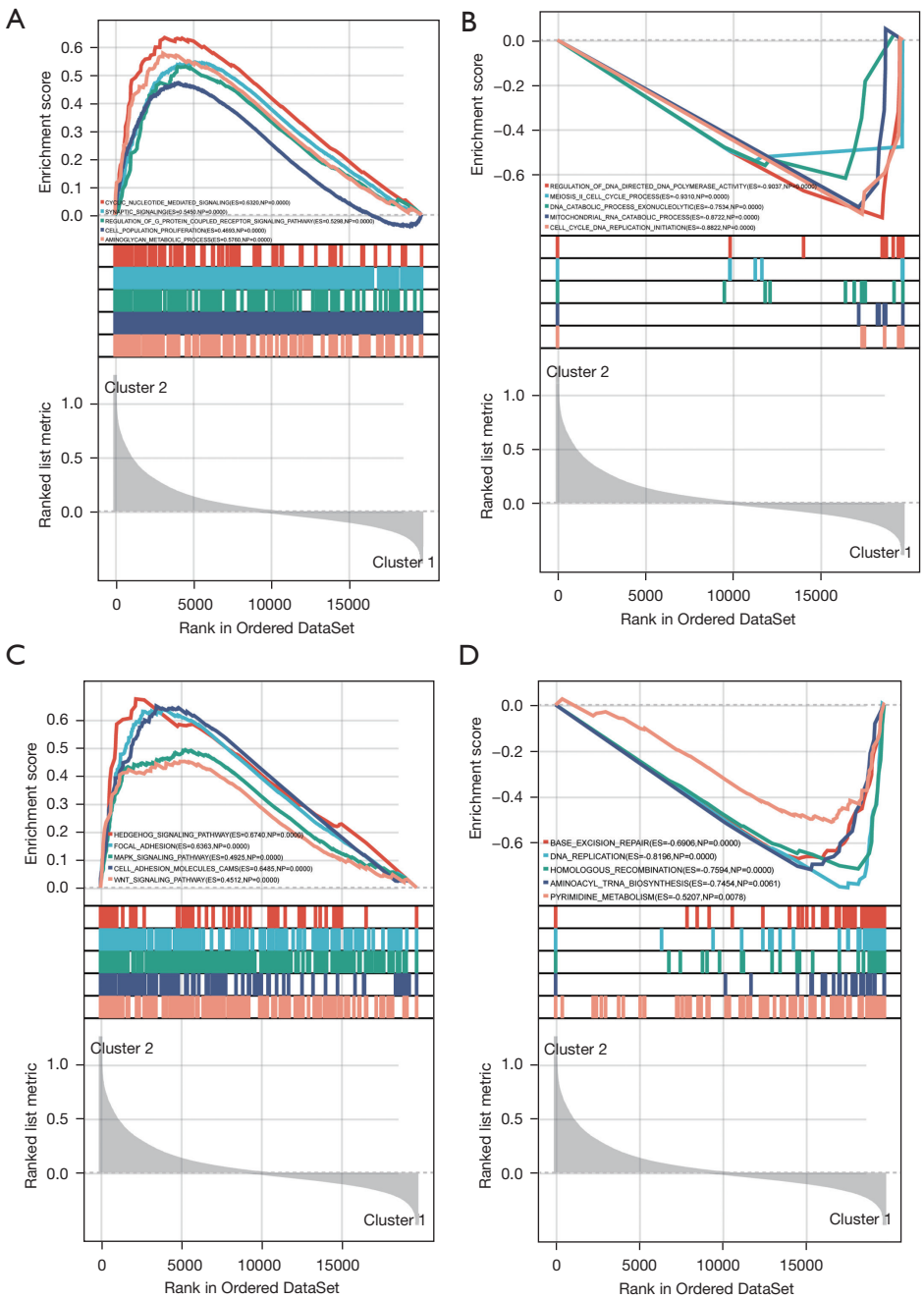


**Figure 4** GSEA functional enrichment analysis among different subtypes. (A) Cluster 2 enrichment results in GOBP. (B) Cluster 1 enrichment results in GOBP. (C) Cluster 2 enrichment results in KEGG. (D) Cluster1 enrichment results in KEGG. GSEA, gene set enrichment analysis; GOBP, Gene Ontology Biological Process; KEGG, Kyoto Encyclopedia of Genes and Genomes.

polymerase_activity (ES =–0.9037), etc. (*Figure 4A,4B*). The main enriched KEGG pathways were hedgehog_signaling_pathway (ES =0.6740), focal_adhesion (ES =0.6363), base_excision_repair (ES =–0.6906), etc. (*Figure 4C,4D*).

### *Analysis of somatic mutation among different clusters*

To investigate the somatic mutation frequencies among the different STAD clusters, the different mutational patterns between the 186 samples of cluster 1 and the 186 samples of

 

cluster 2 were observed. The splice site, nonsense mutation, nonstop mutation, in frame del, missense mutation, frame shift ins and frame shift del were significantly different between clusters (*Figure 5A*). Moreover, the frequencies of missense mutations were the largest in both cluster 1 and cluster 2. Somatic mutation signatures of SNVs, INS, SNPs and DELs were significantly different between clusters (*Figure 5B,5C*). Additionally, the gene mutation of the patients in clusters 1 and 2 is shown in *Figure 5D,5E*. The TTN was the highest gene mutation in the patients of clusters 1 and 2 (*Figure 5D,5E*). A total of 31 differentially mutated genes were selected between cluster 1 and cluster 2, including PSD, HDAC4 and INADL (*Figure 5F*).

### *Immune microenvironment analysis*

To study immune cell infiltration in patients with different clusters, the proportions of 22 immune cells in the 189 samples of cluster 2 and the 186 samples of cluster 1 were calculated. Among them, 152 samples of cluster 2 and 106 samples of cluster 1 were screened for further exploration. There were eight immune cells that were significantly different between clusters, including T cells follicular helper, T cells CD4 memory activated, macrophages M2, T cells CD4 memory resting, monocytes, dendritic cells activated, mast cells resting and eosinophils (*Figure 6A*). Additionally, the immune score, stromal score and estimate score were calculated in the different clusters and there were significant differences in the two clusters (*Figure 6B-6E*).

### *Sensitivity analysis of immunotherapy and predictive analysis of chemotherapeutics*

The patients in cluster 2 were sensitive to CTLA4 inhibitor treatment with P=0.02 (*Figure 7A*). Furthermore, of the top five drugs are shown in *Figure* 7, AP.24534, BX.795, Midostaurin, WO2009093927 and CCT007093 were significantly higher in cluster 1 than in cluster 2 (*Figure 7B-7F*).

### *Screening for prognostic genes and prognostic analysis*

A total of 1,734 DEGs were obtained from clusters 1 and 2: 1,427 upregulated DEGs and 307 downregulated DEGs (*Figure 8A*). Next, three prognostic genes (*AOX1*, *NNMT* and *PTGIS*) were acquired from the intersection of the DEGs and DE-NMRGs (*Figure 8B*). In addition, the overall survival (OS) of *AOX1* (P=0.02) (*Figure 8C*), *NNMT* (P=5e−04) (*Figure 8D*) and *PTGIS* (P=0.012) (*Figure 8E*) were different between the high and low expression groups.

### *qRT-PCR*

We performed qRT-PCR on a normal cell line (GES-1) and cancer cell lines (HGC-27, NCI-N87 and SNU-1) to verify the expression of the prognostic genes. The expressions of *PTGIS*, *NNMT* and *AOX1* were the same as the results of the bioinformatics analysis. The expressions of *PTGIS* and *AOX1* were higher in the normal cell line (GES-1) than in the cancer cell lines (HGC-27, NCI-N87 and SNU-1), but that of *NNMT* was lower (*Figure 9*).

## Discussion

STAD has high incidence and mortality rates, accounting for 95% of GC cases. It is the fifth most common malignancy worldwide and the fourth leading cause of cancer death worldwide (1). Because the disease is often diagnosed late, its prognosis is poor (25,26). Many studies have shown that people with GC have alterations in $NAD^+$ metabolism-related molecules or chemicals (13,27), but no studies have reported the $NAD^+$ metabolic signatures with regard to GC prognosis.

$NAD^+$ is a key coenzyme in redox processes and an enormously critical aspect of energy metabolism (8). $NAD^+$ can directly and indirectly affect several essential biological activities, including metabolic pathways, DNA repair, chromatin remodeling, cellular senescence, and immune cell function (28,29). Studies have indicated that $NAD^+$ levels play a role in cancer progression through multiple signaling pathways affecting DNA repair and cellular defense (30,31). ATP and $NAD^+$ produced by cells in the tumor microenvironment can be transformed to adenosine by CD38 ecto-NADase and CD39 ecto-ATPase, hence lowering T cell function and inhibiting tumor immunity (32). NADK has been found to be cancer-promoting, and inhibition of this enzyme lowers tumor cell proliferation and xenograft growth *in vivo* (33). Studies have found that nicotinamide mononucleotide (NMN) supplementation in combination with PD-L1 antibodies significantly inhibits tumor progression *in vivo*, suggesting that NAD supplementation may be a promising therapeutic strategy for the treatment of drug-resistant tumors (13). Oxaliplatin attenuates the NAD/NADH ratio by blocking tumor-associated NADH oxidase (tNOX), consequently

 

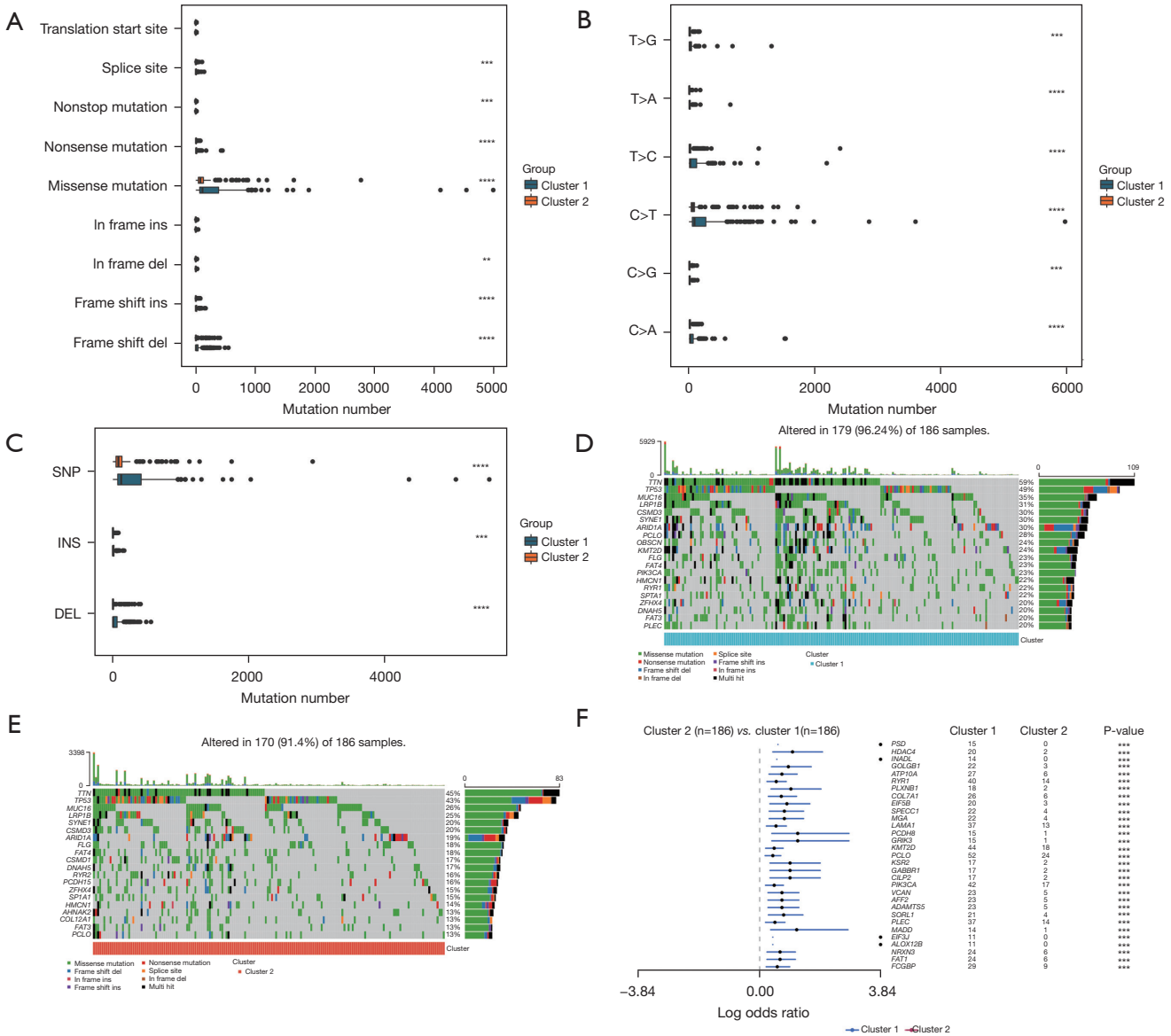


**Figure 5** Differences in cell mutations between different subtypes. (A) Boxplots of somatic mutation frequencies among different subtypes. (B) Boxplot of somatic mutation characteristics of SNV among different subtypes. (C) Boxplot of somatic mutation characteristics of SNP, INS and DEL among different subtypes. (D) Waterfall plot of the top 20 genes with mutation frequency in cluster 1, the central plot shows the types of mutations in each sample, the right plot demonstrates the mutation frequency (Y-axis) of each gene (X-axis), and the upper plot exhibits the frequency in mutations (Y-axis) of each sample (X-axis). (E) Waterfall plot of the top 20 genes with mutation frequency in cluster 2, the central plot shows the types of mutations in each sample, the right plot demonstrates the mutation frequency (Y-axis) of each gene (X-axis), and the upper plot exhibits the frequency in mutations (Y-axis) of each sample (X-axis). (F) Forest map of differentially mutated genes among different subtypes. **, P<0.01; ***, P<0.001; ****, P<0.0001. SNV, single nucleotide variant; SNP, single nucleotide polymorphism; INS, insertions; DEL, deletion.

 

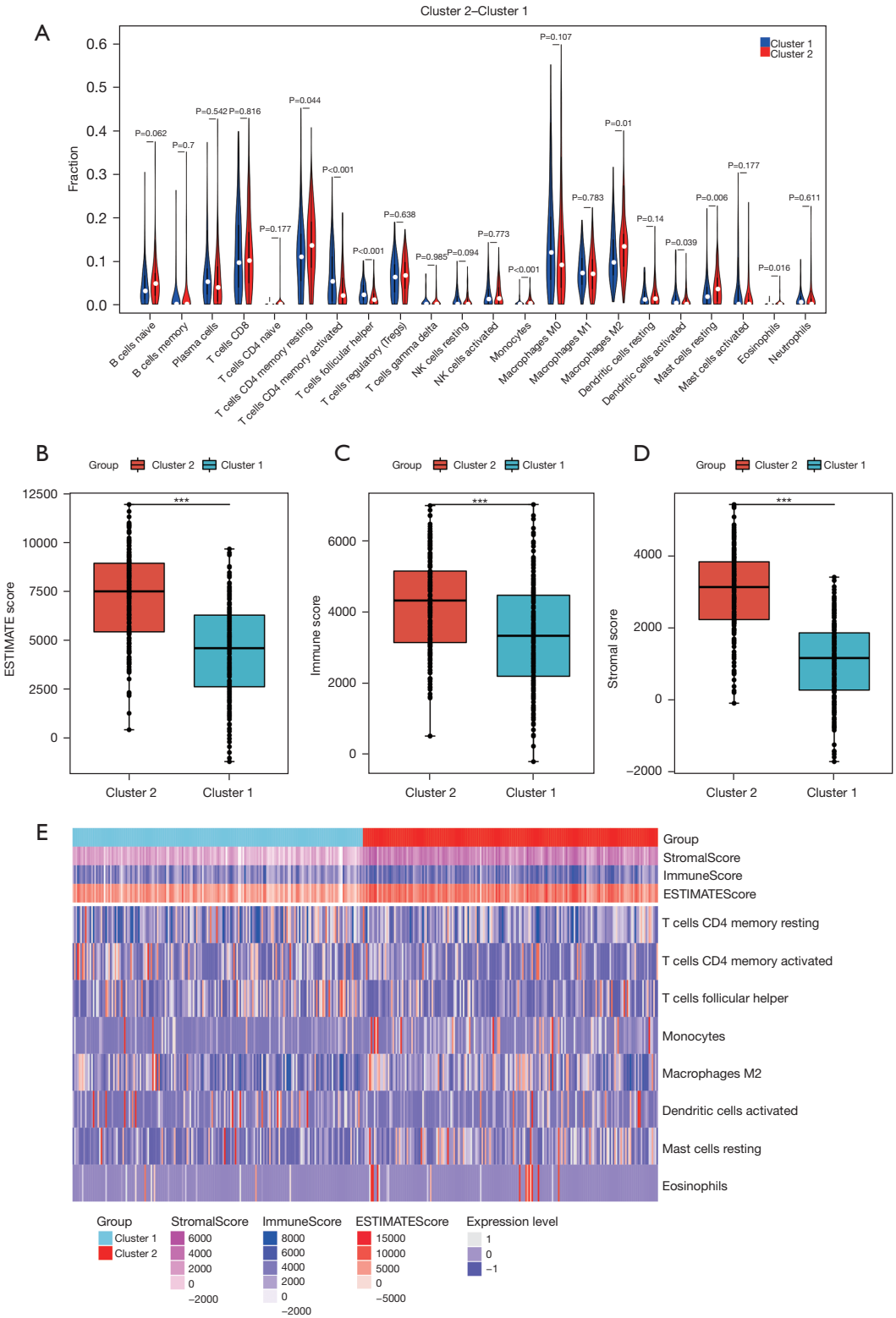


**Figure 6** Immune microenvironment analysis. (A) Violin plot of 22 immune cell infiltration abundances among different subtype groups. (B) Estimate score. (C) Immune score. (D) Stromal score. (E) Heatmap of differential immune cell expression in different subtypes. ***, P<0.001.

 

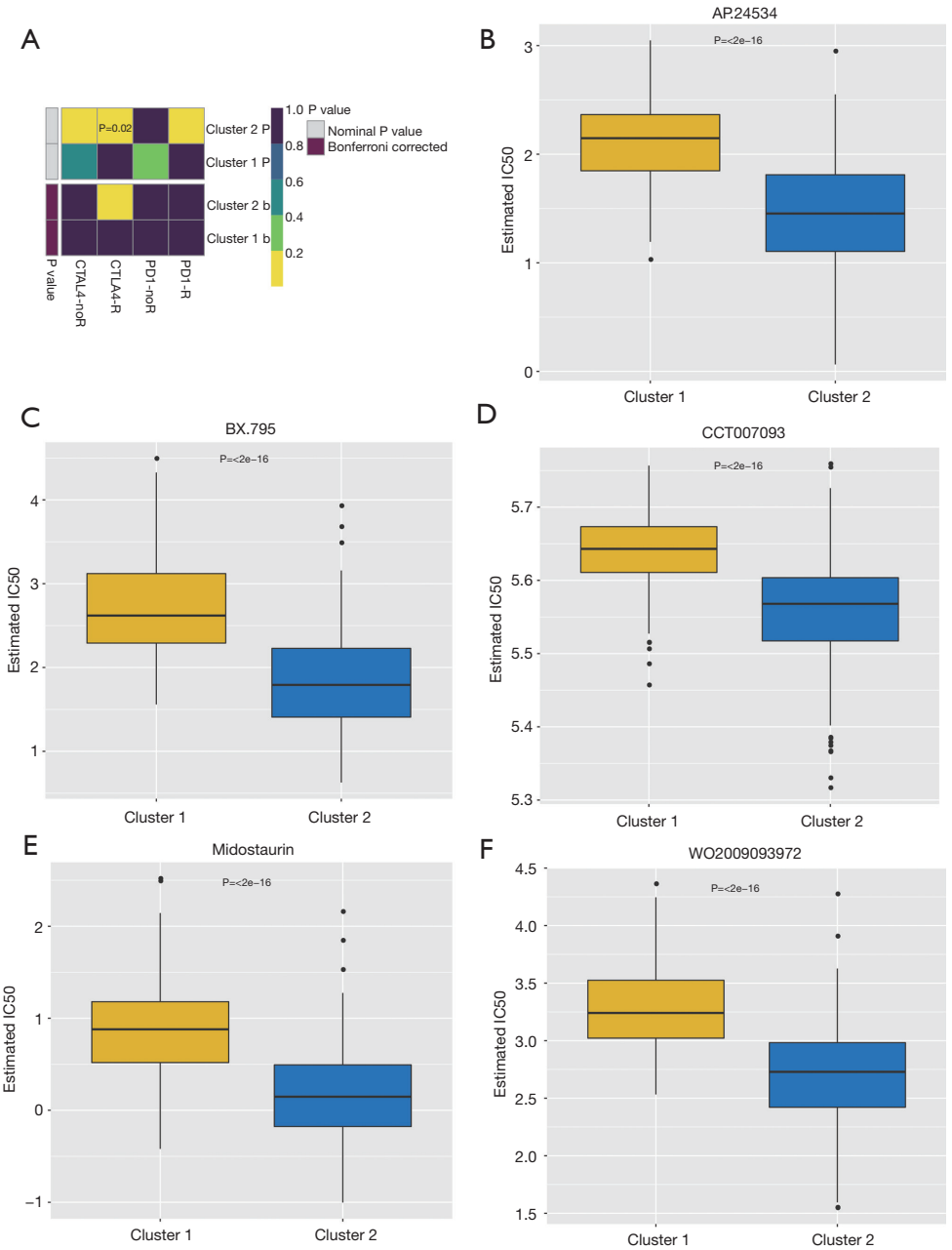


**Figure 7** Differences between subtypes. (A) Heatmap of immunotherapy sensitivity in different subtypes. (B) Predicted AP.24534 IC50 in different subtypes. (C) Predicted BX.795 IC50 in different subtypes. (D) Predicted CCT007093 IC50 in different subtypes. (E) Predicted Midostaurin IC50 in different subtypes. (F) Predicted WO2009093972 IC50 in different subtypes.

boosting p53 acetylation and death of GC cells (34). Liu *et al.* found that suppression of NAMPT function promoted apoptosis in GC cells and improved effector CD8+ T cell function (27). Therefore, an in-depth understanding of the roles of NMRGs in tumor development and elucidation of these molecular mechanisms are of enormous value for cancer therapy targeting NAD+ and its metabolites.

In this study, we carried out molecular stratification analysis based on NMRGs to evaluate the relationship between different clusters and the prognosis of STAD. Finally, qRT-PCR was utilized to evaluate the expression of key prognostic genes in human gastric adenocarcinoma

 

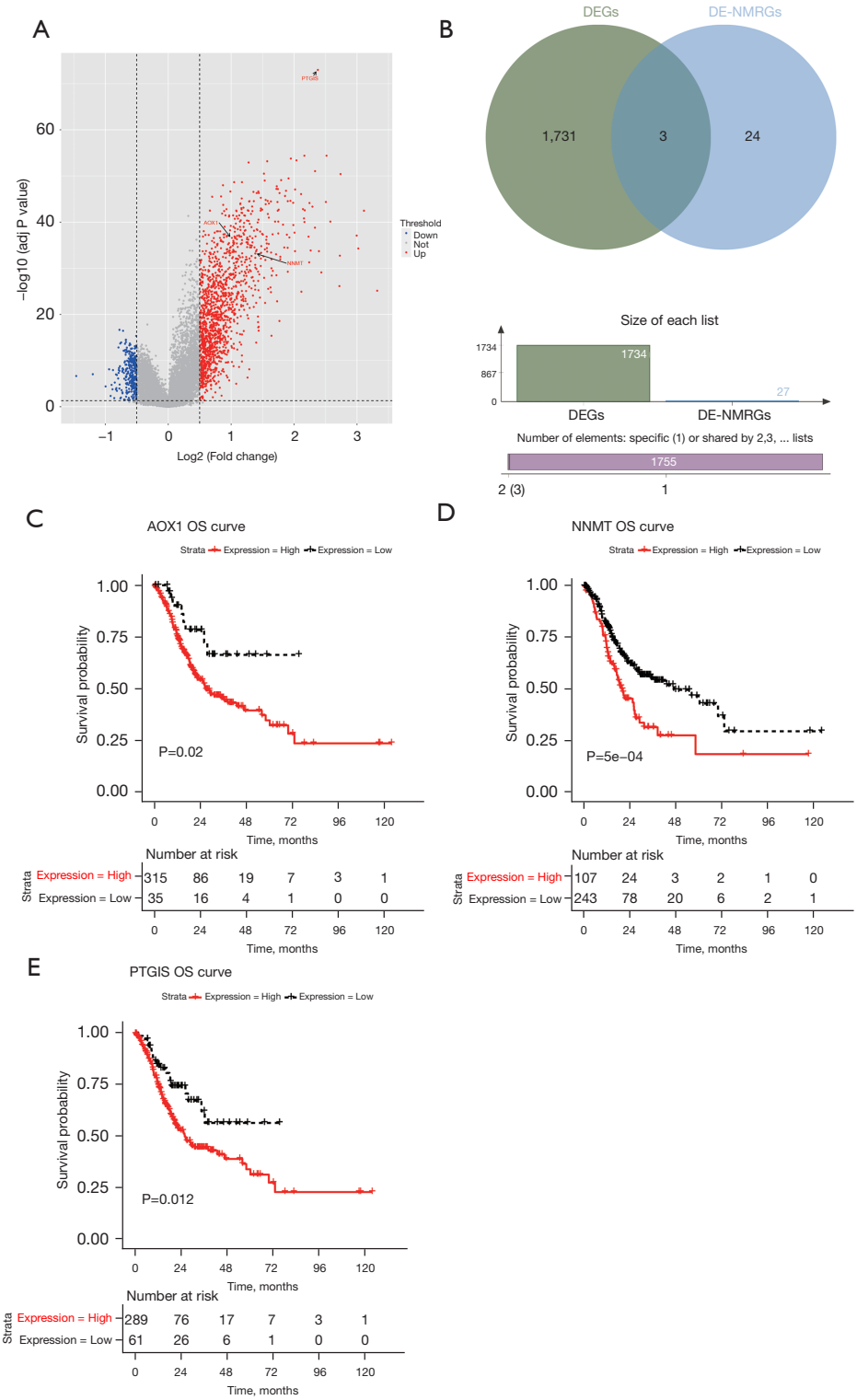


**Figure 8** Analysis of differential genes. (A) Volcano plot of differential genes between different subtypes. (B) Venn diagram of key genes. (C) Kaplan-Meier survival analysis of patients with high or low expression of *AOX1*. (D) Kaplan-Meier survival analysis of patients with high or low expression of *NNMT*. (E) Kaplan-Meier survival analysis of patients with high or low expression of *PTGIS*. DEG, differentially expressed gene; DE-NMRG, differentially expressed NAD$^+$ metabolism-related gene; NAD$^+$, nicotinamide adenine dinucleotide; OS, overall survival.

 

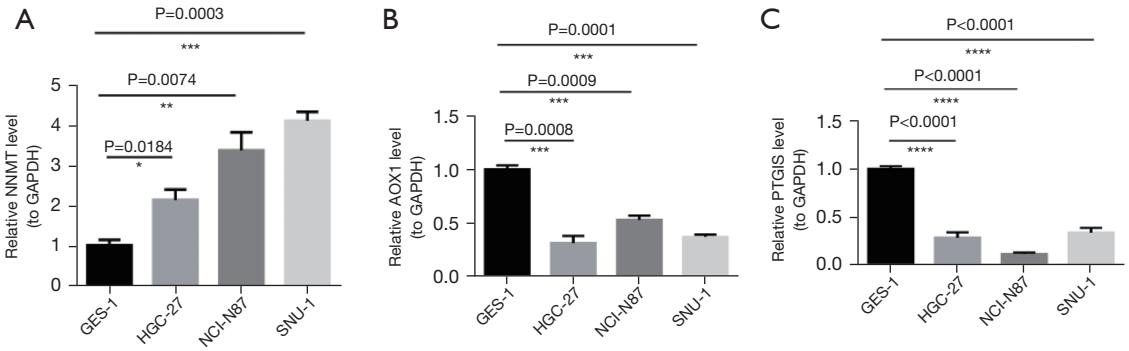


**Figure 9** Gene expressions in different cell lines. (A) *NNMT*. (B) *AOX1*. (C) *PTGIS*. *, P<0.05; **, P<0.01; ***, P<0.001; ****, P<0.0001. GAPDH, glyceraldehyde-3-phosphate dehydrogenase.

cell lines, to further comprehend the *in vivo* differences of STAD patients with different survival rates. *AOX1*, *NNMT* and *PTGIS* are considered to be three key genes associated with STAD prognosis among the NMRGs. The NNMT catalytic reaction is primarily the removal of precursor molecules in the pathway of $NAD^+$ production (12). NNMT methylates NAM to MNAM (8), thus playing a central regulatory role in the metabolism of the cancer-associated fibroblast differentiation and cancer progression in the stroma (35). Both knockdown and pharmacological inhibition of NNMT have been found to lead to an increase in $NAD^+$ content (12). Previous research showed that *NNMT* expression was substantially linked with GC stage, and increased stromal *NNMT* expression predicted poor prognosis in GC, which is consistent with our data (36). It is worth noting that Liu *et al.* demonstrated that NNMT directly interacts with TTPAL to activate PI3K/AKT signaling to promote gastric carcinogenesis, hence partaking in cancer proliferation, invasion, metastasis and drug resistance (37). Likewise, AOX1 is one of the key enzymes in tryptophan catabolism, and deletion of *AOX1* may lead to the accumulation of kynurenine and NADP (38,39). Kynurenine can bind to aromatic hydrocarbon (AhR) receptors on immune cells to evade immune responses by tumors (40). In the clinic, AOX1 has been found to be involved in the development and progression of several malignancies, such as bladder, prostate and colorectal cancers (38,41,42). Prostaglandin I2 synthase (*PTGIS*) is a crucial gene for the synthesis of prostaglandin I2 and plays a key role in inflammation and immune modulation (43,44). High expression of *PTGIS* promotes the infiltration of tumor-associated macrophages and T-regulatory cells (Tregs) in the tumor microenvironment, which leads to a worse prognosis in GC patients (44).

We observed that *TTN* had the highest gene mutation frequency in patients with cluster 1 and cluster 2 subtypes, and the missense mutation accounted for the highest proportion of this gene mutation type. Mutations in *TTN*, the gene encoding giant myofilament titin, cause familial dilated cardiomyopathy (45). Study has shown that patients with a high frequency of *TTN* mutations have a better prognosis, which is similar to our results (46). Yang *et al.* found that *TTN* mutations were effective in predicting GC prognosis, tumor mutation burden (TMB), and immunotherapy response (47).

In order to analyze the infiltration of immune cells in patients with various subtypes, we estimated the proportions of 22 categories of immune cells between the two groups and found that eight types were substantially different in distinct subtype groups. In the high-risk group, the infiltration degree of T cells CD4 memory resting, eosinophils, monocytes, macrophages M2, and mast cells resting was higher, while in the low-risk group, the infiltration degree of T cells CD4 memory activated, T cells follicular helper, and dendritic cells activated was higher. This may imply a protective role for activated $CD4^+$ memory T cells and Tfh cells in GC patients. Previous studies have shown that memory T cells can provide protection against GC and are associated with lymph node metastasis in GC (48). Tryptophan catabolism helps tumor cells evade immune responses through accumulated catabolites, prompting the differentiation of $CD4^+$ cells into Tregs (49,50). High levels of $CD4^+$ T cells appear in the early clinical stage and are significantly correlated with the clinical stage of GC (51). NAMPT plays an important role in the differentiation of macrophages to the M2 phenotype, which usually has low NAD levels (49,50). The tumor-associated macrophages in gastric adenocarcinoma are

 

mainly M2 macrophages, which are closely related to the migration and invasion of tumor cells (52). We discovered that increased macrophage M2 infiltration was related to lower survival outcomes in GC patients. Studies by others have also indicated that large concentrations of macrophages predict worse survival results in GC patients (53,54). The foregoing data show that NMRGs may affect the survival rate of GC patients by influencing immune cell infiltration of tumors. Although our results cannot clarify the effects on immune cells, they reveal their association and their effect on prognosis. The association of $NAD^+$ with immune cell infiltration may allow new research to determine the precise mechanisms of immune escape, ultimately inspiring new therapeutic modalities. Interestingly, we observed significant enrichment of pathways related to DNA replication repair and cell cycle regulation in cluster 1 patients. Cancer cell genome instability, favorable for accumulation of mutations and expansion of tumor heterogeneity, and pathways related to DNA replication repair and cell cycle regulation play essential roles in the development of GC (55,56). Therefore, the relationship between $NAD^+$ metabolism and pathways relevant to DNA replication repair and cell cycle regulation in GC merits additional research.

$NAD^+$ has been reported to enhance DNA demethylation (57). $NAD^+$ is also a substrate for polyribose polymerase 1 (PARP1), a nuclear protein that plays a key role in DNA methylation (58). Tumor NAD metabolism mainly regulates DNA demethylation through Tet1-mediated Dnmts, and NAD metabolism regulates and induces PD-L1 expression by controlling DNA demethylation (13). The link between $NAD^+$ and DNA methylation provides a nutritionally guided approach to clinical cancer management.

In our results, patients with the cluster 2 subtype were shown to be sensitive to cytotoxic T lymphocyte-associated protein (CTLA)-4 inhibitor treatment. The CTLA-4 pathway is a key regulator of T cell responses to tissues, coregulating T cell responses with the receptor CD28 (59). The restriction of the CTLA-4 immune response to self-tissue can be relieved by anti-CTLA-4 antibody (60,61). Ipilimumab is a CTLA-4 inhibitor (61,62). In a single-agent trial of ipilimumab in GC patients, doses of 10 mg/kg did not significantly improve patient outcomes (61). In a multicenter randomized controlled study (NCT02872116), nivolumab plus ipilimumab did not significantly improve OS compared with chemotherapy (63). But we did observe that after 12 months, the nivolumab plus ipilimumab group was superior to chemotherapy (63). These findings imply that CTLA-4 inhibitors may have long-term clinically meaningful OS and progression-free survival (PFS) benefits. Our research into genes related to $NAD^+$ metabolism may suggest that in patients who are sensitive to CTLA-4 inhibitors, combination therapy with anti-CTLA-4 and anti-PD-1 antibodies are worth exploring in future research.

However, this study has some limitations. Some of the genes in the dataset were filtered during the microarray quality control phase, making it impossible to analyze all NMRGs. More cohorts with larger samples are needed to validate our findings, and we will continue to focus on the role of these genes in the future.

## Conclusions

This study assessed the role of $NAD^+$ metabolism genes and pathways in STAD and analyzed the relationship between $NAD^+$ metabolism and immune cell infiltration. In addition, we used qRT-PCR to analyze the expression of key prognostic genes in human gastric adenocarcinoma cell lines. Based on our above analysis, the kynurenine metabolic pathway affected by the key gene AOX1 is a potential target for the treatment of gastric adenocarcinoma, and it may be possible to improve the efficacy of gastric adenocarcinoma immunotherapy by inhibiting kynurenine metabolism. The results provide a theoretical basis and reference for further treatment and prognosis of STAD.

## Acknowledgments

*Funding:* This work was supported by grants from the Key Laboratory (Key Laboratory of Spleen and Stomach Diseases Spleen Deficiency Syndrome) of State Administration of Traditional Chinese Medicine.

## Footnote

*Reporting Checklist:* The authors have completed the REMARK reporting checklist. Available at https://jgo.amegroups.com/article/view/10.21037/jgo-22-1092/rc

*Conflicts of Interest:* All authors have completed the ICMJE uniform disclosure form (available at https://jgo.amegroups.com/article/view/10.21037/jgo-22-1092/coif). The authors have no conflicts of interest to declare.

*Ethical Statement:* The authors are accountable for all aspects of the work in ensuring that questions related

 

to the accuracy or integrity of any part of the work are appropriately investigated and resolved. The study was conducted in accordance with the Declaration of Helsinki (as revised in 2013).



## References

1. Sung H, Ferlay J, Siegel RL, et al. Global Cancer Statistics 2020: GLOBOCAN Estimates of Incidence and Mortality Worldwide for 36 Cancers in 185 Countries. CA Cancer J Clin 2021;71:209-49.
2. Bray F, Ferlay J, Soerjomataram I, et al. Global cancer statistics 2018: GLOBOCAN estimates of incidence and mortality worldwide for 36 cancers in 185 countries. CA Cancer J Clin 2018;68:394-424.
3. Luo SS, Liao XW, Zhu XD. Genome-wide analysis to identify a novel microRNA signature that predicts survival in patients with stomach adenocarcinoma. J Cancer 2019;10:6298-313.
4. Katai H, Ishikawa T, Akazawa K, et al. Five-year survival analysis of surgically resected gastric cancer cases in Japan: a retrospective analysis of more than 100,000 patients from the nationwide registry of the Japanese Gastric Cancer Association (2001-2007). Gastric Cancer 2018;21:144-54.
5. Covarrubias AJ, Kale A, Perrone R, et al. Senescent cells promote tissue NAD(+) decline during ageing via the activation of CD38(+) macrophages. Nat Metab 2020;2:1265-83.
6. Hogan KA, Chini CCS, Chini EN. The Multi-faceted Ecto-enzyme CD38: Roles in Immunomodulation, Cancer, Aging, and Metabolic Diseases. Front Immunol 2019;10:1187.
7. Brachs S, Polack J, Brachs M, et al. Genetic Nicotinamide N-Methyltransferase (Nnmt) Deficiency in Male Mice Improves Insulin Sensitivity in Diet-Induced Obesity but Does Not Affect Glucose Tolerance. Diabetes 2019;68:527-42.
8. Covarrubias AJ, Perrone R, Grozio A, et al. NAD(+) metabolism and its roles in cellular processes during ageing. Nat Rev Mol Cell Biol 2021;22:119-41.
9. Coleman MP, Höke A. Programmed axon degeneration: from mouse to mechanism to medicine. Nat Rev Neurosci 2020;21:183-96.
10. Chini CCS, Zeidler JD, Kashyap S, et al. Evolving concepts in NAD(+) metabolism. Cell Metab 2021;33:1076-87.
11. Verdin E. NAD+ in aging, metabolism, and neurodegeneration. Science 2015;350:1208-13.
12. Katsyuba E, Romani M, Hofer D, et al. NAD+ homeostasis in health and disease. Nat Metab 2020;2:9-31.
13. Lv H, Lv G, Chen C, et al. NAD(+) Metabolism Maintains Inducible PD-L1 Expression to Drive Tumor Immune Evasion. Cell Metab 2021;33:110-127.e5.
14. Li C, Zhu Y, Chen W, et al. Circulating NAD+ Metabolism-Derived Genes Unveils Prognostic and Peripheral Immune Infiltration in Amyotrophic Lateral Sclerosis. Front Cell Dev Biol 2022;10:831273.
15. Gómez-Rubio V. ggplot2 - Elegant Graphics for Data Analysis (2nd Edition). Journal of Statistical Software, Book Reviews 2017;77:1-3.
16. Wilkerson MD, Hayes DN. ConsensusClusterPlus: a class discovery tool with confidence assessments and item tracking. Bioinformatics 2010;26:1572-3.
17. Mosmann T. Rapid colorimetric assay for cellular growth and survival: application to proliferation and cytotoxicity assays. J Immunol Methods 1983;65:55-63.
18. Suárez-Fariñas M, Lowes MA, Zaba LC, et al. Evaluation of the psoriasis transcriptome across different studies by gene set enrichment analysis (GSEA). PLoS One 2010;5:e10247.
19. Mayakonda A, Koeffler HP. Maftools: Efficient analysis, visualization and summarization of MAF files from large-scale cohort based cancer studies. BioRxiv 2016. doi: 10.1101/052662.
20. Chen B, Khodadoust MS, Liu CL, et al. Profiling Tumor Infiltrating Immune Cells with CIBERSORT. Methods Mol Biol 2018;1711:243-59.
21. Guindon S, Dufayard JF, Lefort V, et al. New algorithms and methods to estimate maximum-likelihood phylogenies: assessing the performance of PhyML 3.0. Syst Biol 2010;59:307-21.
22. Kolde R. Pheatmap: pretty heatmaps. R Package Version 2012;1:726.
23. Geeleher P, Cox N, Huang RS. pRRophetic: an R package for prediction of clinical chemotherapeutic response from tumor gene expression levels. PLoS One 2014;9:e107468.

24. Smyth GK. Limma: linear models for microarray data. Bioinformatics and computational biology solutions using R and Bioconductor. New York: Springer, 2005:397-420.
25. Harada K, Yamashita K, Iwatsuki M, et al. Intraperitoneal therapy for gastric cancer peritoneal carcinomatosis. Expert Rev Clin Pharmacol 2022;15:43-9.
26. Sethi NS, Kikuchi O, Duronio GN, et al. Early TP53 alterations engage environmental exposures to promote gastric premalignancy in an integrative mouse model. Nat Genet 2020;52:219-30.
27. Liu HY, Wang FH, Liang JM, et al. Targeting NAD metabolism regulates extracellular adenosine levels to improve the cytotoxicity of CD8+ effector T cells in the tumor microenvironment of gastric cancer. J Cancer Res Clin Oncol 2022. [Epub ahead of print]. doi: 10.1007/s00432-022-04124-9.
28. Yu P, Cai X, Liang Y, et al. Roles of NAD+ and Its Metabolites Regulated Calcium Channels in Cancer. Molecules 2020;25:4826.
29. Zapata-Pérez R, Wanders RJA, van Karnebeek CDM, et al. NAD(+) homeostasis in human health and disease. EMBO Mol Med 2021;13:e13943.
30. Poljsak B, Milisav I. NAD+ as the Link Between Oxidative Stress, Inflammation, Caloric Restriction, Exercise, DNA Repair, Longevity, and Health Span. Rejuvenation Res 2016;19:406-15.
31. Lahiguera Á, Hyroššová P, Figueras A, et al. Tumors defective in homologous recombination rely on oxidative metabolism: relevance to treatments with PARP inhibitors. EMBO Mol Med 2020;12:e11217.
32. Horenstein AL, Quarona V, Toscani D, et al. Adenosine Generated in the Bone Marrow Niche Through a CD38-Mediated Pathway Correlates with Progression of Human Myeloma. Mol Med 2016;22:694-704.
33. Tedeschi PM, Bansal N, Kerrigan JE, et al. NAD+ Kinase as a Therapeutic Target in Cancer. Clin Cancer Res 2016;22:5189-95.
34. Chen HY, Cheng HL, Lee YH, et al. Tumor-associated NADH oxidase (tNOX)-NAD+-sirtuin 1 axis contributes to oxaliplatin-induced apoptosis of gastric cancer cells. Oncotarget 2017;8:15338-48.
35. Eckert MA, Coscia F, Chryplewicz A, et al. Proteomics reveals NNMT as a master metabolic regulator of cancer-associated fibroblasts. Nature 2019;569:723-8.
36. Zhang L, Song M, Zhang F, et al. Accumulation of Nicotinamide N-Methyltransferase (NNMT) in Cancer-associated Fibroblasts: A Potential Prognostic and Predictive Biomarker for Gastric Carcinoma. J Histochem Cytochem 2021;69:165-76.
37. Liu W, Gou H, Wang X, et al. TTPAL promotes gastric tumorigenesis by directly targeting NNMT to activate PI3K/AKT signaling. Oncogene 2021;40:6666-79.
38. Vantaku V, Putluri V, Bader DA, et al. Epigenetic loss of AOX1 expression via EZH2 leads to metabolic deregulations and promotes bladder cancer progression. Oncogene 2020;39:6265-85.
39. Castro-Portuguez R, Sutphin GL. Kynurenine pathway, NAD(+) synthesis, and mitochondrial function: Targeting tryptophan metabolism to promote longevity and healthspan. Exp Gerontol 2020;132:110841.
40. Prendergast GC. Cancer: Why tumours eat tryptophan. Nature 2011;478:192-4.
41. Zhang W, Chai W, Zhu Z, et al. Aldehyde oxidase 1 promoted the occurrence and development of colorectal cancer by up-regulation of expression of CD133. Int Immunopharmacol 2020;85:106618.
42. Li W, Middha M, Bicak M, et al. Genome-wide Scan Identifies Role for AOX1 in Prostate Cancer Survival. Eur Urol 2018;74:710-9.
43. Ershov PV, Mezentsev YV, Kopylov AT, et al. Affinity Isolation and Mass Spectrometry Identification of Prostacyclin Synthase (PTGIS) Subinteractome. Biology (Basel) 2019;8:49.
44. Dai D, Chen B, Feng Y, et al. Prognostic value of prostaglandin I2 synthase and its correlation with tumor-infiltrating immune cells in lung cancer, ovarian cancer, and gastric cancer. Aging (Albany NY) 2020;12:9658-85.
45. Gerull B, Gramlich M, Atherton J, et al. Mutations of TTN, encoding the giant muscle filament titin, cause familial dilated cardiomyopathy. Nat Genet 2002;30:201-4.
46. Liu Y, Cheng L, Huang W, et al. Genome Instability-Related miRNAs Predict Survival, Immune Landscape, and Immunotherapy Responses in Gastric Cancer. J Immunol Res 2021;2021:2048833.
47. Yang Y, Zhang J, Chen Y, et al. MUC4, MUC16, and TTN genes mutation correlated with prognosis, and predicted tumor mutation burden and immunotherapy efficacy in gastric cancer and pan-cancer. Clin Transl Med 2020;10:e155.
48. Xie S, Mo P, Li N, et al. Tumor-Infiltrating Lymphocyte-Based Risk Score for Predicting Prognosis in Gastric Cancer. Front Oncol 2020;10:522015.
49. Navas LE, Carnero A. NAD(+) metabolism, stemness, the immune response, and cancer. Signal Transduct Target Ther 2021;6:2.


 

50. Audrito V, Managò A, Gaudino F, et al. NAD-Biosynthetic and Consuming Enzymes as Central Players of Metabolic Regulation of Innate and Adaptive Immune Responses in Cancer. Front Immunol 2019;10:1720.
51. Zhang R, Li F, Li H, et al. The clinical significance of memory T cells and its subsets in gastric cancer. Clin Transl Oncol 2014;16:257-65.
52. Seeneevassen L, Bessède E, Mégraud F, Lehours P, Dubus P, Varon C. Gastric Cancer: Advances in Carcinogenesis Research and New Therapeutic Strategies. Int J Mol Sci 2021;22:3418.
53. Eissmann MF, Dijkstra C, Jarnicki A, et al. IL-33-mediated mast cell activation promotes gastric cancer through macrophage mobilization. Nat Commun 2019;10:2735.
54. Yu J, Zhang Q, Wang M, et al. Comprehensive analysis of tumor mutation burden and immune microenvironment in gastric cancer. Biosci Rep 2021;41:BSR20203336.
55. Zhang L, Hu D, Huangfu S, et al. DNA Repair and Replication-Related Gene Signature Based on Tumor Mutation Burden Reveals Prognostic and Immunotherapy Response in Gastric Cancer. J Oncol 2022;2022:6469523.
56. Tanabe S, Quader S, Ono R, et al. Cell Cycle Regulation and DNA Damage Response Networks in Diffuse- and Intestinal-Type Gastric Cancer. Cancers (Basel) 2021;13:5786.
57. Chang J, Zhang B, Heath H, et al. Nicotinamide adenine dinucleotide (NAD)-regulated DNA methylation alters CCCTC-binding factor (CTCF)/cohesin binding and transcription at the BDNF locus. Proc Natl Acad Sci U S A 2010;107:21836-41.
58. Ummarino S, Hausman C, Gaggi G, et al. NAD Modulates DNA Methylation and Cell Differentiation. Cells 2021;10:2986.
59. Rowshanravan B, Halliday N, Sansom DM. CTLA-4: a moving target in immunotherapy. Blood 2018;131:58-67.
60. Lingel H, Brunner-Weinzierl MC. CTLA-4 (CD152): A versatile receptor for immune-based therapy. Semin Immunol 2019;42:101298.
61. Bang YJ, Cho JY, Kim YH, et al. Efficacy of Sequential Ipilimumab Monotherapy versus Best Supportive Care for Unresectable Locally Advanced/Metastatic Gastric or Gastroesophageal Junction Cancer. Clin Cancer Res 2017;23:5671-8.
62. Korman AJ, Garrett-Thomson SC, Lonberg N. The foundations of immune checkpoint blockade and the ipilimumab approval decennial. Nat Rev Drug Discov 2022;21:509-28.
63. Shitara K, Ajani JA, Moehler M, et al. Nivolumab plus chemotherapy or ipilimumab in gastro-oesophageal cancer. Nature 2022;603:942-8.

(English Language Editor: K. Brown)

**Cite this article as:** Cai L, Ke C, Lin Z, Huang Y, Wang A, Wang S, Chen C, Zhong C, Fu L, Hu P, Chai J, Zhang H, Zhang B. Prognostic value of nicotinamide adenine dinucleotide (NAD+) metabolic genes in patients with stomach adenocarcinoma based on bioinformatics analysis. J Gastrointest Oncol 2022;13(6):2845-2862. doi: 10.21037/jgo-22-1092

 

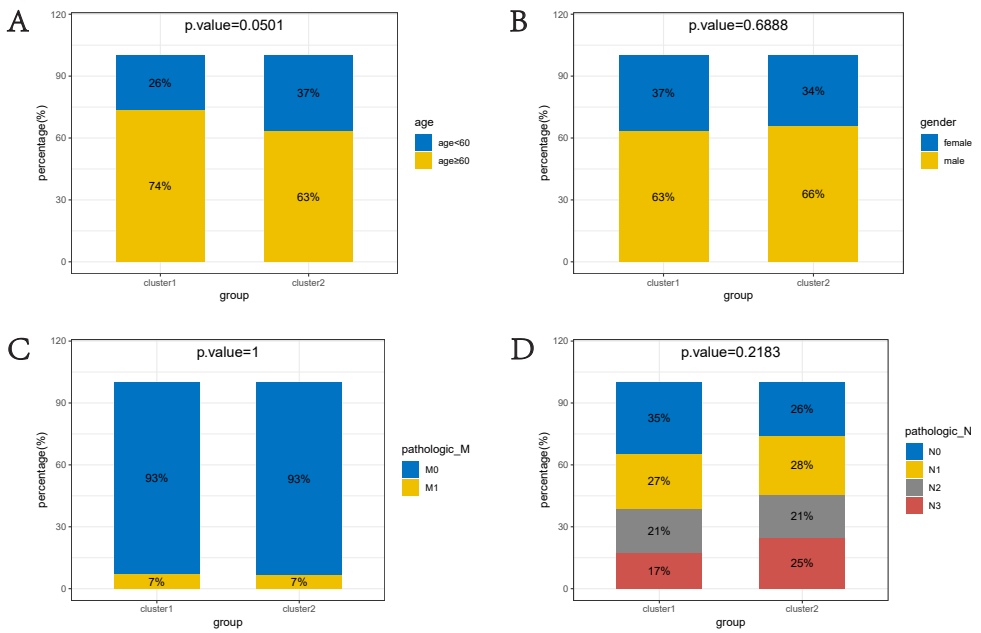


**Figure S1** Comparison of different subtypes with clinical features. (A) Age. (B) Gender. (C) Pathologic M stage. (D) Pathologic N stage.


https://dx.doi.org/10.21037/jgo-22-1092